Growing Neural Gas-based Maximum Torque per Ampere (MTPA) Technique for SynRMs

Angelo Accetta, MEMBER, IEEE
National Research Council of Italy (CNR),
INstitute of Marine engineering (INM)
Palermo, Italy
angelo.accetta@cnr.it

Maurizio Cirrincione, SENIOR MEMBER, IEEE
University of the South Pacific,
School of Engineering,
Laucala Campus, Suva, Fiji
m.cirrincione@ieee.org

Maria Carmela Di Piazza, SENIOR MEMBER, IEEE
National Research Council of Italy (CNR),
INstitute of Marine engineering (INM)
Palermo, Italy
mariacarmela.dipiazza@cnr.it

Giuseppe La Tona, MEMBER, IEEE
National Research Council of Italy (CNR),
INstitute of Marine engineering (INM)
Palermo, Italy
giuseppe.latona@cnr.it

Massimiliano Luna , MEMBER, IEEE
National Research Council of Italy (CNR),
INstitute of Marine engineering (INM)
Palermo, Italy
massimiliano.luna@cnr.it

Marcello Pucci, SENIOR MEMBER, IEEE
National Research Council of Italy (CNR),
INstitute of Marine engineering (INM)
Palermo, Italy
marcello.pucci@cnr.it

***Abstract*— This paper proposes a maximum torque per ampere (*MTPA*) technique specifically developed for Synchronous Reluctance Motors (*SynRMs*). The proposed *MTPA* is based on a self-organizing artificial neural network, called Growing Neural Gas (*GNG*). The *GNG* gas been trained in order to learn the real maximum torque per ampere points of the *SynRM* under test. The proposed *MTPA* has been tested experimentally on a suitably developed test set-up. The obtained experimental results clearly highlight a significant increase of maximum producible torque, with respect to the previously developed *MTPA* techniques.**

Keywords—Synchronous Reluctance Motor (SynRM), Maximum Torque Per Ampere (MTPA), Rotor Oriented Control, Neural Networks (NN), Growing Neural Gas (GNG)

I. INTRODUCTION

High dynamic performance control of Synchronous reluctance motors (*SynRM*) can be achieved exploiting vector control schemes; among these last ones, both rotor-oriented and stator flux-oriented control techniques have been developed [1]-[4]. The non-linear magnetic behavior of the *SynRMs* limits theoretically their dynamic performance. In more details, saturation effects present remarkable differences on the direct (*x*) and quadrature (*y*) axes, Furthermore, cross-saturation phenomena are significant in such machines [5][6]. If the electromechanical conversion has to be performed with maximum efficiency, maximum torque per ampere (*MTPA*) techniques have to be embedded in the control scheme. If the simplification of linearity of the magnetic circuit is assumed, implying constant inductance terms of the model, the *MTPA* problem leads to the classic solution with equal x, y components of the stator current in the rotor reference frame $i_{sx} = |i_{sy}|$ [1]. If the magnetic saturation of the machine is to dealt with, several approaches have been followed. One of the approaches has been proposed in [7], where a set of curves have been traced starting from experimental measurements, giving the relationship between the amplitude of the stator current and its x component, according to different values of load torque. Even [8] and [9] propose MTPA techniques based on the classic relationship $i_{sx} = |i_{sy}|$. Nevertheless, while [9] is based on a classic rotor-oriented vector control, furnishing the reference of i_{sx} as a function of the load torque, [8] proposes a stator flux-oriented control. The magnetic saturation, however, has been neglected in the *MTPA* formulation. A different approach, fully considering the magnetic saturation, has been followed in [10], proposing an algebraic magnetic model based on current versus flux functions. Afterwards, the Brent algorithm is exploited after inverting numerically the magnetic model by the Powell dogleg algorithm. Alternatively, finite element analyses (*FEA*) approaches have been exploited for the optimal torque control [11]; they, however, need a punctual knowledge of the design and construction of the motor More recently, the *MTPA* problem specifically developed for *SynRMs* has been faced up by an analytical formulation accounting for the magnetic saturation of the iron core [12]. This technique is based on a simplified model describing the magnetic saturation of the *SynRM*, derived by a previously developed more detailed magnetic model accounting for both self and cross-saturation [13]. The approach followed in [13] reveals effective and performing in a wide working range of speeds and loads. Specific working region s exist, however, where the MPTA solution obtained with [13] is not optimal; this is the case for high values of the speed and load torque. This paper, trying to overcome the limits of the method in [13] in specific working areas, proposes an *MTPA* based on an intelligent mapping, and specifically on a self-organizing artificial neural network, called Growing Neural Gas (*GNG*) [14] by exploiting the specific capability of the *GNG* to learn complex functions with a limited number of processing units, called neurons. With this aim, a suitable set of off-line experimental tests has been developed to perform the real *MTPA* in the entire working range of the stator current amplitude and rotor speed. Afterwards, the set of measured real *MTPA* working points has been trained off-line with the *GNG*. The recalling phase of the *GNG* has been employed on-line to implement an intelligent look-up table performing the real *MTPA* task. The proposed *MTPA* has been tested experimentally on a suitably developed test set-up.

II. THE GNG-BASED MTPA

A. Retrieval of the real MTPA

In the following, the procedure that has been devised to experimentally retrieve the real *MTPA*, in the entire working range of the machine, will be described. The control system implemented in the *SynRM* drive is the rotor-oriented control, where the classic *MTPA* has been further integrated; specifically, the rotor oriented control has been operated in current control. On the other hand, the *PMSM* (Permanent Magnet Synchronous Motor) drive adopted as an active load has been operated in speed control. The procedure adopted in each working point is the following. A constant rotor reference speed has been given to the *PMSM* drive. Starting from zero, the reference speed is then modified in order to the entire drive working range. As for the *SynRM* drive, starting from the working condition at $\delta = \pi/4$ corresponding to the classic *MTPA*, the amplitude of the stator current $|\mathbf{i}_s|$ has been maintained constant while the angle δ had been continuously varied, step by step, in both directions, till the maximum electromagnetic torque is achieved. Given the stator current amplitude $|\mathbf{i}_s|$ and speed ω_r under test, the torque angle δ_{max} and the corresponding maximum electromagnetic torque t_{emax} have been then memorized as the real *MTPA*. Such a methodology has been applied to the *SynRM* drive described in section 3; the obtained experimental results are provided in Fig. 1, that shows the experimental points (red) describing, for the *SynRM* drive under test, the relationship between the steady-state real maximum torque versus the stator current amplitude and the rotor speed. The same plot provides even the surface interpolating the experimental measurements. It can be observed that the maximum producible torque increases quickly with the stator current amplitude, while it decreases slightly for increasing values of the rotor speed, as expected.

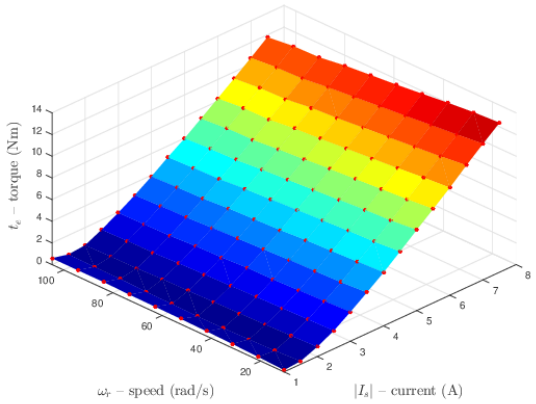

Fig. 1. Steady-state maximum producible torque vs rotor speed and stator current amplitude

B. GNG Training of the real MTPA

The growing neural gas (*GNG*) is a particular kind of self-supervised neural network inspired by the self-organizing map (*SOM*). It is a relatively simple algorithm for finding optimal representations of data by using feature vectors. The algorithm has been called "*neural gas*" because of the dynamics of the feature vectors during the adaptation process, which distribute themselves like a gas within the data space. A number of variants of the neural gas algorithms exist in the literature; *Fritzke* [14] describes the growing neural gas (*GNG*) as an incremental network model that learns topological relations by using a "Hebb-like learning rule" only; unlike the neural gas, *GNG* has no parameters that change over time and it is capable of continuous learning. The main idea of the *GNG* is to add new units (neurons) to an initially small network in a growing structure. With this approach, the network topology is generated incrementally and has a dimensionality that depends on the input data and may vary locally. Two phases should be distinguished, namely, the training and the recalling. The training phase is performed off-line and can be run on a regular PC: in this phase, specifically, the experimental data related to the real *MTPA* have been learnt by the *GNG*. The recalling phase is performed on-line and it builds an intelligent mapping of the data; a limited number of processing units is able, therefore, to represent a higher number of experimental data points. This phase has been implemented on-line on the same DSP on which the control system runs. In the following, the algorithms of both the training and recalling phases are described.

Training Phase

A neuron of the *GNG* is represented, in this case, by the 3-dimensional vector of its weights, whose variables are respectively the direct component of the stator currents, the total amplitude of the stator current vector and the rotor speed. Besides its weights, each neuron is characterized by some links between itself and other close neurons. The links represent the topological relationship between the neurons and they are labeled with a value indicating the age. This parameter measures how well the connected neurons represent all the input data. Indeed, after a certain age, links are removed and then neurons are deleted because they do not correctly represent the data, being considered outliers.

The complete algorithm of the *GNG* is summarized in the following steps.

1. Define the maximum number of neurons n_{max} and the maximum number of the epochs n_{epmax}.
2. Start with two neurons a and b with random weights $\boldsymbol{w}_a$ and $\boldsymbol{w}_b$ in $\Re^n$.
3. Present a sample $\boldsymbol{\xi}$ from the training set, obeying some unknown probability density function $P(\boldsymbol{\xi})$.
4. Find the nearest neuron $\mathbf{s_1}$ and the second nearest neuron $\mathbf{s_2}$. The closeness of the neurons is established based on the Euclidean distance.
5. Increment the age of all edges emanating from $\mathbf{s_1}$.
6. Add the squared distance between the input signal and the nearest neuron in the input space to a local counter variable:
$$\Delta error(\mathbf{s}_1) = \left\| \mathbf{w}_{s_1} - \boldsymbol{\xi} \right\|^2 .$$
7. Move $\mathbf{s_1}$ and its direct topological neighbors towards $\boldsymbol{\xi}$ by fractions ε_b and ε_n , of the total distance, respectively:

$$\begin{cases} \Delta \mathbf{w}_{s_1} = \varepsilon_b \left(\xi - \mathbf{w}_{s_1} \right) \\ \quad \ldots \\ \Delta \mathbf{w}_n = \varepsilon_n \left(\xi - \mathbf{w}_n \right) \end{cases}$$

for all direct neighbors n of $\mathbf{s_1}$.

8. If $\mathbf{s_1}$ and $\mathbf{s_2}$ are connected with an edge, set the age of this edge to zero. In this way, frequently activated neurons remain young. If this edge does not exist, create it.
9. Remove edges with an age larger than a_{max}. If this results in points with no emanating edges, remove them.
10. If the number of samples presented so far is an integer multiple of a parameter λ and the number of the created neurons n is lower than its maximum n_{max}, create a new neuron as follows:
    a. Determine the neuron $\boldsymbol{q}_l$ with the maximum accumulated error.
    b. Insert a new neuron $\boldsymbol{r}$ halfway between $\boldsymbol{q}$ and its neighbour $\boldsymbol{f}$, and remove the original edge between $\boldsymbol{q}$ and $\boldsymbol{f}$.
    c. Decrease the error variables of $\boldsymbol{q}$ and $\boldsymbol{f}$ by multiplying them by a constant α. Initialize the error variable of $\boldsymbol{r}$ with the new value of the error variable of $\boldsymbol{q}$.
11. Decrease all error variables by multiplying them by a constant d.
12. If a stopping criterion, for example the number of epochs n_{ep} is equal to its maximum n_{epmax}, is not yet fulfilled go to step 2.

Fig. 2 shows the flow chart of the training algorithm of the *GNG*.

Recalling Phase

The recall algorithm is as follows:

1. Present the input vector $\boldsymbol{\xi}_i$.
2. Compute the K Euclidean distances D_k between the vector $\boldsymbol{\xi}_i$ and the weights $\mathbf{w}_k$ of the K neurons.
3. Sort out the D_k's in increasing order and select the corresponding first P neurons.
4. Compute the estimated output $\mathbf{y}_i$ by:

$$y_i = \sum_{k=1}^{P} \frac{w_k}{D_k} \Big/ \sum_{k=1}^{P} \frac{1}{D_k}$$

Before training *GNG*, the experimental data shown in Fig. 1 have been pre-processed offline. The pre-processing yields the total amplitude of the stator current from its cartesian components, in order to find the experimental mapping describing the relationship between the direct component of the stator current in the rotor reference frame i_{sx} versus the total amplitude of the stator current vector $|I_s|$ as well as the rotor speed ω_r. This process results in Fig. 3, which shows the steady-state experimental mapping between i_{sx} versus $|I_s|$and ω_r (black squares), the related interpolating surface and the set of neurons generated at the end of the GNG training (violet circles). Specifically, 60 neurons have been found able to represent the entire set of experimental data. It can be observed that the neurons properly cover the entire *MTPA* surface, confirming the correctness of its training process.

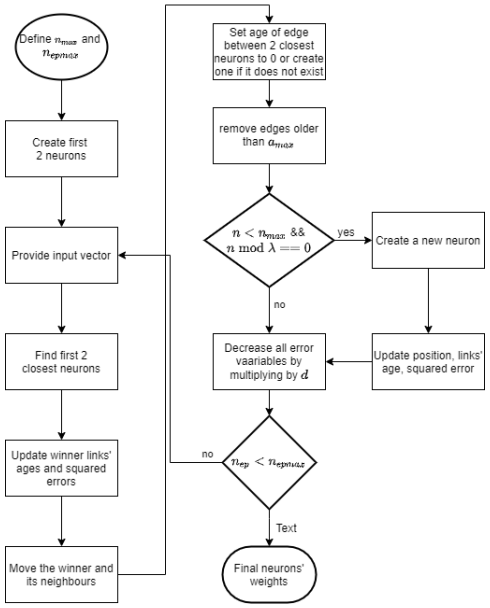

Fig. 2. Flow chart of the *GNG* training algorithm

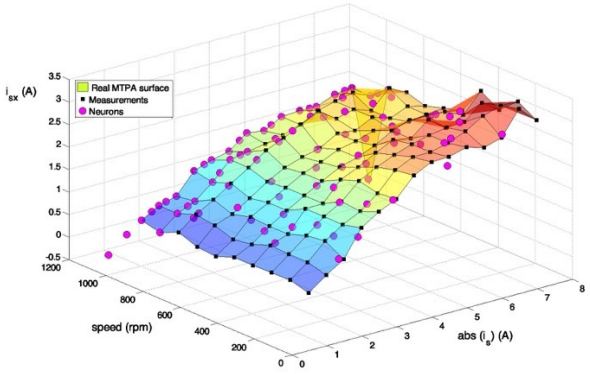

Fig. 3. Steady-state experimental mapping between i_{sx} vs $|I_s|$and ω_r, interpolating surface and neuron generated with the *GNG* training

III. Test Set-up

The employed test set-up consists of a *SynRM* motor *ABB 3GAL092543-BSB*. The *SynRM* is supplied by a Voltage Source Inverter (VSI) with insulated gate bipolar transistor (*IGBT*) modules, *Semikron SMK 50 GB 123,* driven by a space-vector Pulse Width Modulation technique (*SV-PWM*) with PWM frequency set to 5 kHz.

The *SynRM* drive has been controlled by adopting a rotor oriented control [1]-[4]. The proposed *MTPA* technique has been embedded into this control scheme.

Both the adopted PWM and the control techniques have been implemented on a dSPACE card (DS1103) with a PowerPC

604e at 400 MHz and a floating-point DSP TMS320F240. The sampling time of the control system has been set to 10 kHz. The *SynRM* motor is mechanically coupled to a torque controlled *PMSM* drive working as active load. Fig. 4 shows the photo of the *SynRM* drive test set-up.

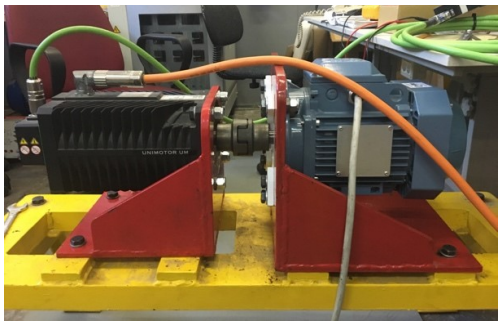

Fig. 4. Photograph of the Experimental Set-up

IV. Experimental Results

The proposed GNG-based MTPA technique has been implemented on the test set-up described in Section 3, integrating it in the rotor-oriented vector control scheme [1]-[4].

The proposed *MTPA* has been also compared experimentally with two MTPAs proposed by the scientific literature, namely the classic *MTPA* technique and the MTPA accounting for the magnetic saturation in [12]. Two experiments have been carried out, whose results are fully described in the following.

As for the first experiment, a speed step reference of 50 rad/s at no load has been provided to the *SynRM* drive. When the drive is at speed steady-state, a step load torque of amplitude 10 Nm (close to the machine rated torque) has been applied and then released. The load torque variation has been obtained providing a corresponding reference torque to the torque-controlled *PMSM* drive adopted as active load. Fig. 5 shows the reference and measured speeds during such a test. The measured speed quickly tracks its reference, exhibiting a very low rising time. After the application of the step load torque as well as after its release, the reaction of the speed control loop to the effect of the load is to be observed; as a final results, the measured speed is driven by the control system towards its reference. Fig. 6 shows the corresponding waveforms of i_{sx}, i_{sy}. Specifically, i_{sy} presents a stepwise waveform, with peaks occurring at each load application/release, as expected. At the same time, i_{sx} increases with i_{sy}, according to the experimental mapping in Fig.3. Finally, Fig. 7 shows the electromagnetic and load torques obtained during this test. The electromagnetic torque presents a shape similar to that of i_{sy}, and it highlights the same peaks; it tracks the load properly during the load application/release.

As for the second experiment, a speed constant reference of 50 5rad/s has been provided to the *SynRM* drive; when the drive is working at constant speed, a set of increasing step load torques is then applied, ranging from 0 to 10 Nm. Figs. 8 to 10 show the same kind of waveforms as in test 1. These figures show the correct behavior of the control system in general, as well as of the proposed *MTPA* specifically. In particular. It is to be noted that the speed control loop reacts to each load torque step, with the measured speed properly tracking its reference. The current waveforms show an increase of i_{sy} in response to each increase of the load torque. Correspondingly, i_{sx} increases with i_{sy}, according to the experimental mapping in Fig.3. Finally, the electromagnetic torque tracks the load one, as expected. Fig. 11 shows two surfaces describing the increase of the maximum producible torque Δt_e versus the stator current amplitude $|\mathbf{i}_s|$ and speed ω_r. Δt_e represents the difference between the real maximum torque and the torque obtained with the proposed *MTPA*, for the first surface, or the maximum torque obtainable with the classic one, for the second surface. Fig. 11 shows, superimposed, the experimental points and the interpolating surfaces. It can be observed that, for all the values of the stator current amplitudes and rotor speeds, the increase of the maximum producible torque with the proposed *MTPA* is very high. In particular, as for the MTPA in [13], this increase is relevant only for high values of load torque and speed, getting a maximum of approximately 15%. On the contrary, such an increase is relevant in the entire range of load torque and speed for the classic *MTPA*, getting a maximum of approximately 38.5%.

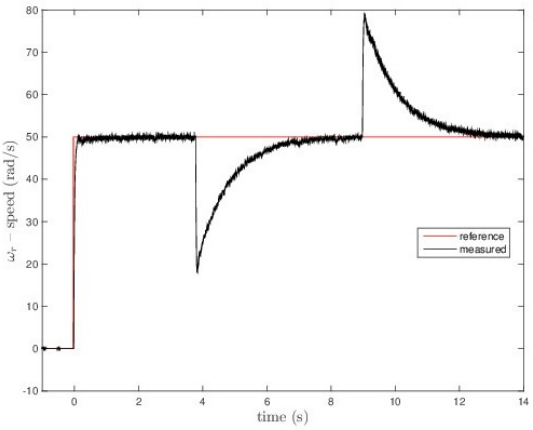

Fig. 5. Reference and measured speed with the GNG-based MTPA during the start-up test - experiment

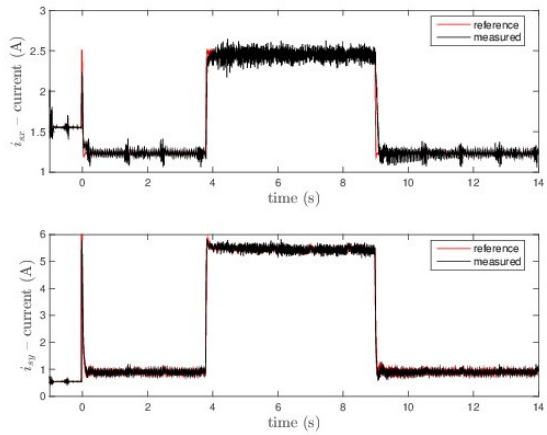

Fig. 6. i_{sx} , i_{sy} with the GNG-based MTPA during the start-up test - experiment

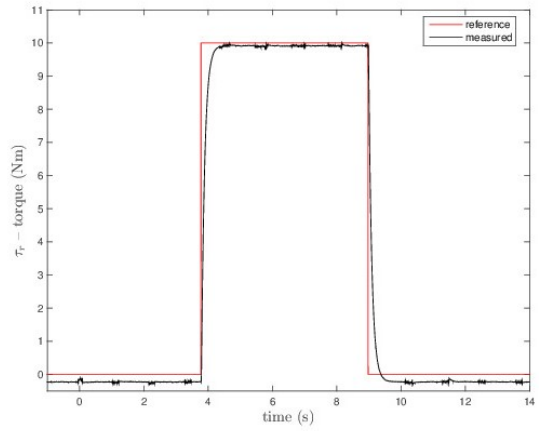

Fig. 7. Reference and measured speed with the GNG-based MTPA during the step load test - experiment

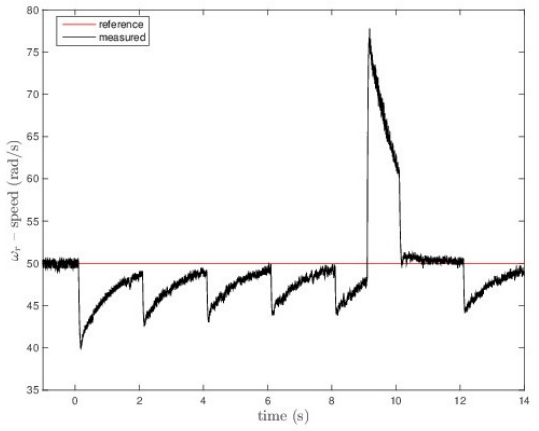

Fig. 8. Electromagnetic and load torques with the GNG-based MTPA during the start-up test - experiment

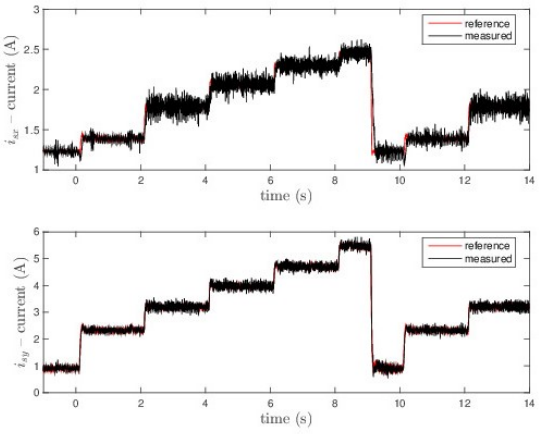

Fig. 9. i_{sx} , i_{sy} with the GNG-based MTPA during the step load test - experiment

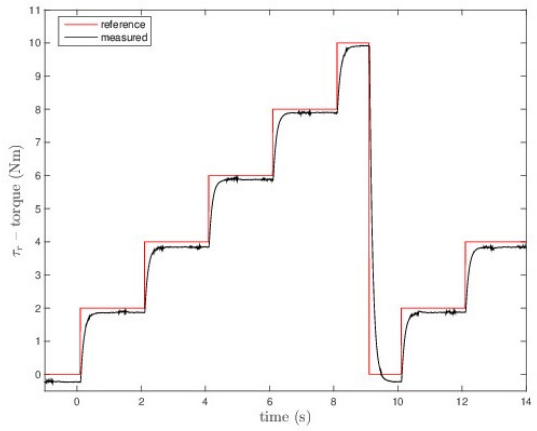

Fig. 10. Electromagnetic and load torques with the GNG-based MTPA during the step load test - experiment

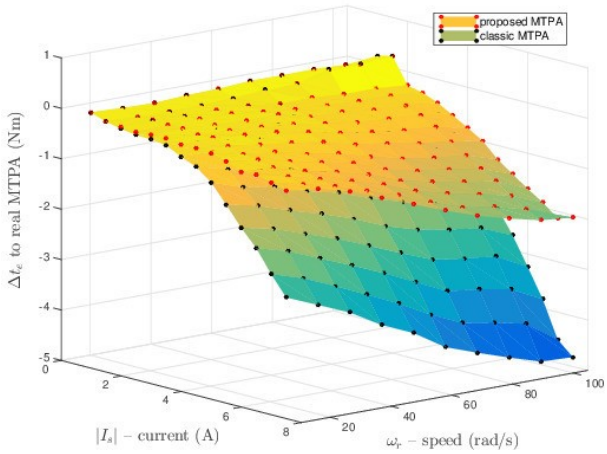

Fig. 11. Steady-state increase of maximum producible torque vs rotor speed and stator current amplitude

V. Conclusions

This paper proposes a maximum torque per ampere (*MTPA*) technique specifically developed for Synchronous Reluctance Motors (*SynRMs*). The proposed MTPA is based on a specific self-organizing artificial neural network, called Growing Neural Gas (*GNG*). The proposed *MTPA* has been tested experimentally on a suitably developed test set-up. Experimental results clearly show that the proposed *MTPA* technique permits a significant increase of maximum producible torque, with respect to a previously developed *MTPA* techniques.

References

[1] P. Vas, Sensorless Vector and Direct Torque Control. Oxford Science, 1998.

[2] L. Xu, X. Xu, T. A. Lipo, and D. W. Novotny, "Vector control of a synchronous reluctance motor including saturation and iron loss," *IEEE Trans. Ind. Appl.*, vol.27, no.5, pp.977–985, Sep./Oct. 1991.

[3] R. E. Betz, R. Lagerquist, M. Jovanovic, T. J. E. Miller, and R. H. Middleton, "Control of synchronous reluctance machines," *IEEE Trans. Ind. Appl.*, vol.29, no.6, pp.1110–1122, Nov./Dec. 1993.

[4] A. Vagati, M. Pastorelli, and G. Franceschini, "High performance control of synchronous reluctance motors," *IEEE Trans. Ind. Appl.*, vol.33, no. 4, pp. 983–991, Jul./Aug. 1997.

[5] A. Vagati, M. Pastorelli, F. Scapino, G. Franceschini, "Impact of cross saturation in synchronous reluctance motors of the transverse-laminated type," *IEEE Trans. Ind. Appl.*, vol. 36, n. 4, Jul./Aug. 2000, pp. 1039–1046.

[6] Y. Li, Z. Q. Zhu, D. Howe, and C. M. Bingham, "Modeling of cross-coupling magnetic saturation in signal-injection-based sensorless control of permanent-magnet brushless AC motors," *IEEE Trans. Magn.,* vol. 43, no. 6, Jun. 2007, pp. 2552–2554.

[7] E. M. Rashad, T. S. Radwan, and M. A. Rahman, "A maximum torque per ampere vector control strategy for synchronous reluctance motors considering saturation and iron losses," *in Conf. Rec. IEEE IAS Annu. Meeting,* Oct. 2004, pp. 2411–2417.

[8] Y. Inoue, S. Morimoto, and M. Sanada, "A Novel Control Scheme for Maximum Power Operation of Synchronous Reluctance Motors Including Maximum Torque Per Flux Control," *IEEE Trans. Ind. Appl.*, vol.47, no. 1, pp. 115–121, Jan./Feb. 2011.

[9] J. Bonifacio, and R. M. Kennel, "On Considering Saturation and Cross-Coupling Effects for Copper Loss Minimization on Highly Anisotropic Synchronous Machines," *IEEE Trans. Ind. Appl.*, vol.54, no. 5, pp. 4177–4185, Sept./Oct. 2018.

[10] H. A. A. Awan, Z. Song, S. E. Saarakkala, M. Hinkkanen, "Optimal Torque Control of Saturated Synchronous Motors: Plug-and-Play Method," *IEEE Trans. Ind. Appl.*, vol.54, no. 6, pp. 6110–6120, Nov./Dec. 2018.

[11] H. W. de Kock, A. Rix, and M. J. Kamper, "Optimal torque control of synchronous machines based on finite-element analysis," *IEEE Trans. Ind. Electron.*, vol. 57, no. 1, pp. 413–419, Jan. 2010.

[12] A. Accetta, M. Cirrincione, M. C. Di Piazza, G. La Tona, M. Luna, M. Pucci, "Analytical Formulation of a Maximum Torque per Ampere (MTPA) Technique for SynRMs Considering the Magnetic Saturation", *IEEE Transaction on Industry Application,* vol. 56, no. 4, pp. 3846-3854, 2020.

[13] A. Accetta, M. Cirrincione, M. Pucci, A. Sferlazza, "A Saturation Model of the Synchronous Reluctance Motor and its Identification by Genetic Algorithms", *2018 IEEE Energy Conversion Congress and Exposition (ECCE)*, 2018, pp. 4460 – 4465.

[14] B. Fritzke, "Growing Cell Structures – a self-organizing network for unsupervised and supervised learning", *Neural Networks,* 7(9), 1994, pp. 1441-1460.

•